

# A Reusable Cobalt Catalyst for Reversible Acceptorless Dehydrogenation and Hydrogenation of N-Heterocycles

Garima Jaiswal,<sup>[b]</sup> Murugan Subaramanian,<sup>[a]</sup> Manoj K. Sahoo,<sup>[b]</sup> and Ekambaram Balaraman<sup>\*[a]</sup>

The development of robust catalytic systems based on base-metals for reversible acceptorless dehydrogenation (ADH) and hydrogenation of feedstock chemicals is very important in the context of 'hydrogen storage'. Herein, we report a highly

efficient reusable cobalt-based heterogeneous catalyst for reversible dehydrogenation and hydrogenation of N-heterocycles. Both the ADH and the hydrogenation processes operate under mild, benign conditions.

## Introduction

N-heteroaromatics are extensively used in the synthesis of natural products, bioactive molecules, and pharmaceuticals.<sup>[1]</sup> Besides, these molecules show profound applications in material science and as Liquid Organic Hydrogen Carriers (LOHCs) in fuel cells.<sup>[2]</sup> Owing to this, a sustainable catalytic approach for their synthesis is highly demanding (Scheme 1). Hence, catalytic dehydrogenation reaction of partially saturated N-heterocycles to N-heteroaromatics is highly desirable and paid much attention in contemporary science.<sup>[3–5]</sup> Conventionally, dehydrogenation reactions were performed using the stoichiometric amount of strong oxidants such as DDQ, peroxides, iodates, chromium (IV) reagents and metal oxides, which often produce excess hazardous waste.<sup>[6]</sup> An alternative to these toxic oxidants, pressurized air or oxygen was used as the sole oxidant.<sup>[7–12]</sup> Catalytic dehydrogenation can also be performed in presence of hydrogen acceptors such as sterically hindered alkenes, and ketones.<sup>[13]</sup> The overall process is redox neutral and does not involve net hydrogen evolution; however, the byproduct is the stoichiometric amount of sacrificial organic waste. In this context, catalytic acceptorless dehydrogenation reaction with the liberation of hydrogen gas is the preferred and promising route for many synthetic transformations and indeed hydrogen is expected to play a key role as an energy carrier in the future.<sup>[14–15]</sup>

Notably, removal of hydrogen atoms from adjacent atomic centers of a saturated organic molecule is highly challenging and thermodynamically uphill process. Recent DFT calculations and experimental results showed that the presence of a nitrogen atom in the cyclic system makes the dehydrogenation process more accessible by lowering the activation energy.<sup>[16]</sup>

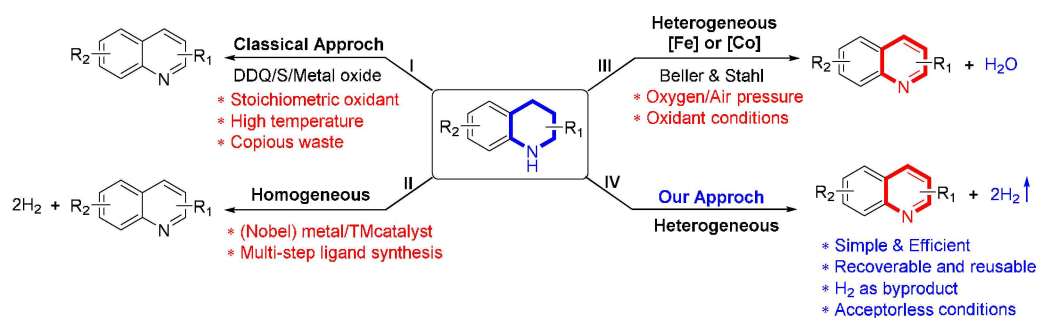
Indeed, it is highly challenging and demanding to develop an efficient and robust, reusable catalytic system to explore its catalytic performance for the ADH of N-heterocycles.<sup>[17]</sup>

Significant contributions have been made in the transition-metal catalyzed ADH reactions of N-heterocyclic compounds by various research groups using well-defined metal complexes under homogeneous conditions.<sup>[18–19]</sup> Despite all, the use of precious metal complexes with multistep synthesized ligands, and difficulties in reuse of the soluble catalysts are the major concerns. Alternatively, heterogeneous catalysis could be a better option over homogeneous catalysis. The significant advantage of heterogeneous catalyst is its capability for easy separation from the reaction mixture and durability of recycling for several runs. Notably, several heterogeneous catalytic systems have been well-documented for the oxidative dehydrogenation of N-heterocycles using air or oxygen as a sole oxidant.<sup>[20]</sup> Indeed, a robust, reusable catalyst for the ADH reaction of N-heterocycles remains an essential goal in chemical research. In a continuous effort to discover first-row transition metal catalysts for sustainable catalysis,<sup>[21]</sup> we have focused our attention on heterogeneous cobalt catalyst.<sup>[22]</sup> Notably, a seminal work reported by the research group of Beller and Stahl for the oxidative dehydrogenation of N-heterocycles to N-aromatics using air/oxygen as the oxidant.<sup>[12a–b]</sup> It is noteworthy that the activity of non-noble metal nanoparticles can be controlled by M:L composition, nature of carbon support, pyrolysis temperature and finally the microstructure of the nanomaterial.<sup>[23]</sup> Gratifyingly, the newly synthesized cobalt nanocatalyst showed superior activity in the ADH reaction of partially saturated N-heterocycles to N-heteroaromatics with the liberation of H<sub>2</sub> gas. The present nano-catalyst performs excellently with a five-run recycling test. In the context of 'hydrogen storage', the microscopic reversible hydrogenation reaction is also equally important. Despite notable advancement in the development of catalytic ADH and hydrogenation of N-heterocycles, systems that utilize a single transition-metal catalyst for both processes are rarely studied.<sup>[17b,18a,19a,d–e,24–25]</sup> We have also successfully demonstrated the hydrogenation of N-heteroarenes to the corresponding N-heterocycles catalysed by the same cobalt nano-catalyst.

[a] M. Subaramanian, Prof. E. Balaraman  
Department of Chemistry  
Indian Institute of Science Education and Research Tirupati (IISER-Tirupati)  
Tirupati – 517507 (India)  
E-mail: eb.raman@iisertirupati.ac.in

[b] G. Jaiswal, M. K. Sahoo  
Organic Chemistry Division  
CSIR-National Chemical Laboratory (CSIR-NCL)  
Dr. Homi Bhabha Road, Pune – 411008 (India)

Supporting information for this article is available on the WWW under <https://doi.org/10.1002/cctc.201900367>



Scheme 1. Overview of the present ADH work.

## Results and Discussion

### Preparation and Characterization of Catalysts

The active heterogeneous cobalt catalyst for the ADH of **1a** was synthesized by our previously reported pyrolysis technique.<sup>[21]</sup> Firstly, *in-situ* generated Co-Phen complex (Co(acac)<sub>3</sub>:1,10-phenanthroline = 1:1) was deposited on exfoliated graphene oxide support and pyrolyzed at 800 °C for 4 h under argon atmosphere. The Co-Phen@C catalytic material has been characterized thoroughly using PXRD, TEM, SEM, XPS, ICP and Raman spectroscopy analysis. The PXRD pattern (Figure 1) of

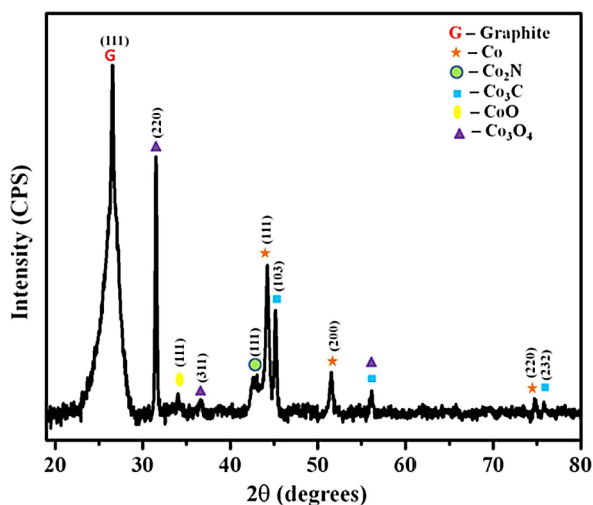


Figure 1. PXRD spectra of Co-Phen@C.

Co-Phen@C shows sharp peaks for Co<sub>3</sub>C, Co<sub>2</sub>N, and Co<sub>3</sub>O<sub>4</sub> phases. In the PXRD, there is a broad peak in the 2θ range 42–47 degree which is due to intermixed phases of Co<sub>3</sub>C and Co<sub>2</sub>N. The formation of Co<sub>3</sub>C and Co<sub>2</sub>N can be understood by the thermal decomposition of nitrogen-rich 1,10-phenanthroline ligand in the proximity of metal atoms that aggregate to form the cobalt carbide and cobalt nitride nanoparticles. Notably, the peak corresponding to Co<sub>3</sub>C was slightly shifted to the higher angle which can be attributed to lattice shrinkage.<sup>[26]</sup> Indeed,

peak broadening in PXRD suggests that nanoparticles are smaller in size.

The microstructure of Co-Phen@C was analyzed using Transmission Electron Microscopy (TEM). The TEM images of Co-Phen@C shows the cobalt nanoparticles were supported and distributed throughout the graphene sheets and having a size in the range of 10–50 nm (Figure 2). However, the majority of nanoparticles were in the range of 20–30 nm as shown in the histogram Figure 2a. Indeed, few particles of size 100–300 nm

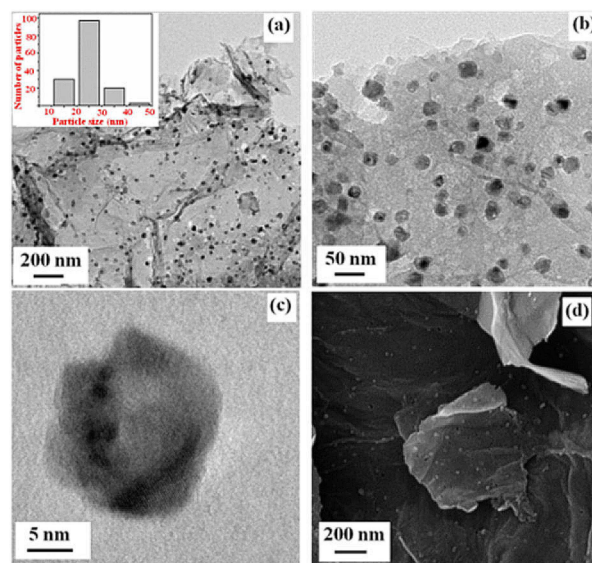


Figure 2. (a) TEM image of Co-Phen@C at the scale of 200 nm, (b) 50 nm, (c) 5 nm, and (d) SEM image of Co-Phen@C (Histogram for the particle size distribution in the inset of Figure 2a).

and some agglomerated particles were also observed. Scanning electron microscopy (SEM) image in Figure 2d also confirms well-separated cobalt nanoparticles on the graphene support. It is clear from the Figure 2 that most of the nanoparticles were spherical in nature and well distributed on graphene support.

To verify the crystalline nature of the nanoparticles, the selected area electron diffraction (SAED) patterns were obtained (Supporting information Figure S4). The ring-like diffraction pattern in SAED image indicates that the particles are partially

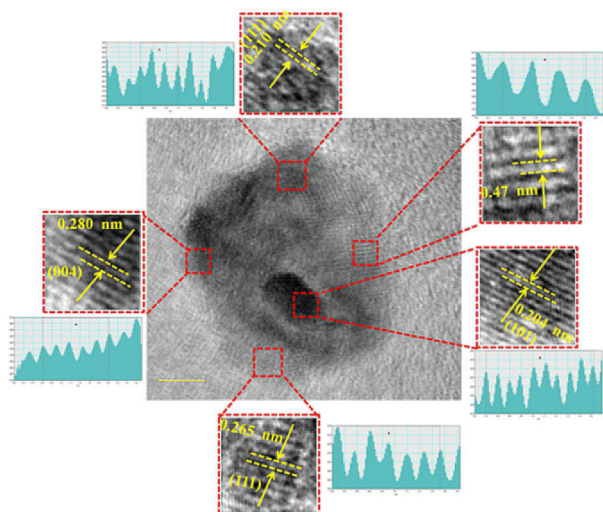


Figure 3. HRTEM image of Co-Phen@C.

crystalline in nature. The bright ring arises due to reflection from (111) plane of  $\text{Co}_2\text{N}$  and (232) of  $\text{Co}_3\text{C}$  planes. The HRTEM images in Figure 3 further verified the various phases present in the Co-Phen@C. In the HRTEM image, interplanar distance of 2.10 Å corresponds to the (111) crystal plane of  $\text{Co}_2\text{N}$ , 4.68 Å corresponds to 111 plane of  $\text{Co}_3\text{O}_4$ . However, few phases were not seen in the PXRD, may be due to low-intensity. The interplanar distance of 2.04 Å corresponds to the d spacing of (111) plane of metallic cobalt phase and 2.82 Å corresponds to the d spacing of (220) plane of  $\text{Co}_3\text{O}_4$ . The HRTEM image clarifies that center of the nanoparticles mainly consists of metallic cobalt and cobalt nitride; while at the ambient

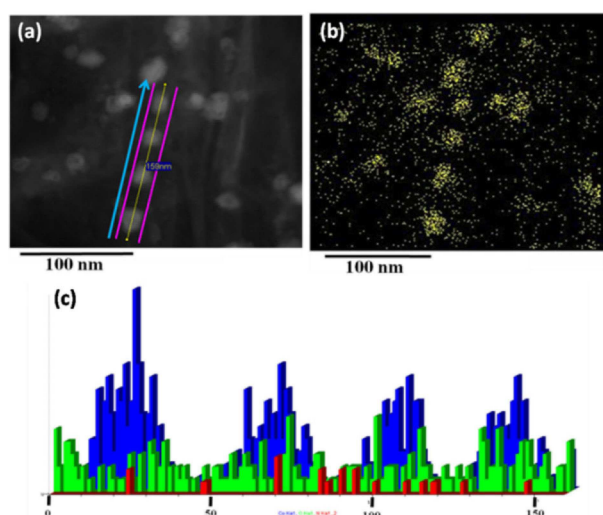


Figure 4. (a) STEM image of Co-Phen@C, bright spots represent the cobalt nanoparticles supported on graphite. (b) Cobalt mapping of Co-Phen@C in which yellow spots represent cobalt nanoparticles. (c) Line profile of Cobalt (blue), Oxygen (green) and Nitrogen (red) passing through a line (yellow color in Figure 4a).

conditions the surface of the nanoparticles got oxidized to cobalt oxides.

Elemental mapping performed on high-angle annular dark-field scanning transmission electron microscopy (HAADF-STEM) mode further supports the distribution of Co across the graphene (Figure 4).

To determine the elements present in the catalytic material and the oxidation state of the cobalt X-ray photoelectron spectra (XPS) analysis was performed in which carbon, nitrogen, oxygen and cobalt metal were detected.<sup>[27]</sup> The two peaks Co 2p<sub>3/2</sub> and Co 2p<sub>1/2</sub> positioned at 780.63 and 795.98 eV in the Co 2p spectrum in (Figure 5a) are attended by two projecting shake-up satellite peaks (786.2 and 800.3 eV) which noticeably validate the presence of the CoO phase.<sup>[28–29]</sup>

Interaction of cobalt metal with nitrogen and carbon is also supported by the N1s spectra and C1s spectra (Supporting information Figure S2). The Figure 5b clearly illustrates that the successful incorporation of nitrogen into the graphitic support and interaction with the cobalt metal. The appearance of specific N1s peak component at 399.6 and 402.6 eV confirms the existence of pyrrolic and graphitic nitrogen motifs<sup>[30]</sup> in the catalyst. The presence of cobalt nitride is further supported by the XPS analysis which is in accordance with the PXRD data. The C1s spectra further support the metal interaction with the graphite support and nitrogen incorporation in the graphite.<sup>[31]</sup>

The presence of Co and N was further confirmed by the Energy-Dispersive X-ray Spectroscopy (EDAX) spectrum (Supporting information Figure S5) taken in the area is shown in Figure 2a of the TEM image, and determined to be 4.57% Co, 4.79% N, 3.25% O, and 86.5% C. The content was also determined by CHN analysis and revealed an atomic ratio of C, H, N, are 76.3%, 1.2%, and 1.46%, respectively and well matches with the EDAX analysis. To determine the cobalt content in Co-Phen@C, inductively coupled plasma optical emission spectrometry (ICP-AES) was performed and found to be 4.3 wt%.

## Catalytic Results

After complete characterization of Co-Phen@C, firstly we have investigated the catalytic activity for the ADH reaction of N-heterocycles. We have chosen 1,2,3,4-tetrahydroquinoline **1a** as

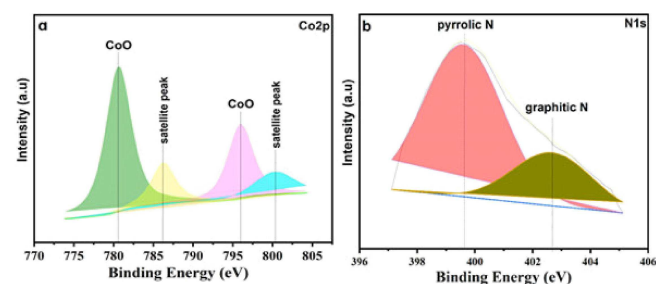


Figure 5. X-ray photoelectron spectra (XPS) of Co-Phen@C (a) Cobalt, (b) Nitrogen.

the model substrate for ADH reaction and studied the effect of each component such as catalyst, solvent, and base (Table 1). After careful screening, we found that substrate **1a** in presence of a catalytic amount of Co-Phen@C, and *t*-BuOK as a base under argon atm gave the dehydrogenated product **2a** in 93% isolated yield (Table 1, entry 1). Notably, the generation of hydrogen gas was qualitatively analyzed on gas chromatography. Under the similar catalytic conditions in a closed system a poor yield of **2a** (41% yield) was obtained and this result suggests the necessity of removal of hydrogen gas from the reaction system (Table 1, entry 2). The base *t*-BuOK was found to be the optimal base for this catalytic transformation. Thus, the reaction in absence of *t*-BuOK or with other bases such as K<sub>2</sub>CO<sub>3</sub> or KOH resulted in a moderate yield of **2a** (Table 1, entries 3–5). We believe that the strong base *t*-BuOK accelerates the substrate binding to the catalyst surface by activating the N–H bond of **1a**. Notably, control experiments indicate that there is no involvement of a radical type mechanism. From a variety of solvents screened, *n*-decane was found to be optimal for the present ADH reaction (Table 1, entries 1, 6–7). At lower reaction temperature, the product yield decreased drastically; hence, the temperature at 150 °C is essential for this transformation (Table 1, entry 8). When the reaction was carried out

in absence of Co-Phen@C there is no formation of **2a** was observed (Table 1, entry 9). It is noteworthy that the other conventional supports and various nitrogen-based ligands didn't yield the desired product in good yields (Table 1, entries 11–17). Beller and Stahl's catalysts gave unsatisfactory results under our optimized conditions (Table 1, entries 18–19). This experiment highlights the robustness of the present catalytic system for ADH reaction of **1a**.

With the optimized reaction conditions in hand, next we have investigated the scope of various partially saturated N-heterocycles (Table 2). Thus, 1,2,3,4-tetrahydroquinolines (THQs)

Table 1. Optimization of the reaction conditions.<sup>[a]</sup>

Entry	Catalyst	Variation from the initial conditions	Conversion of <b>1a</b> <sup>[b]</sup> [%]	Yield of <b>2a</b> <sup>[b]</sup> [%]
1	Co-Phen@C	none	99	97 (93) <sup>c</sup>
2	Co-Phen@C	closed system	48	41 <sup>c</sup>
3	Co-Phen@C	without <i>t</i> BuOK	60	52
4	Co-Phen@C	K <sub>2</sub> CO <sub>3</sub> instead of <i>t</i> BuOK	42	37
5	Co-Phen@C	KOH instead of <i>t</i> BuOK	24	15
6	Co-Phen@C	CH <sub>3</sub> CN instead of <i>n</i> -decane	30	22
7	Co-Phen@C	toluene instead of <i>n</i> -decane	60	50
8	Co-Phen@C	at 80 °C	38	32
9	–	without Co-Phen@C	3	0
10	Co(acac) <sub>3</sub> /Phen	under homogeneous condition	8	trace <sup>d</sup>
11	Co-Phen@SiO <sub>2</sub>	none	36	22
12	Co-Phen@Al <sub>2</sub> O <sub>3</sub>	none	26	20
13	Co-Phen@TiO <sub>2</sub>	none	32	27
14	Co-Bipy@C	none	65	58 (49) <sup>c</sup>
15	Co-Py@C	none	55	51
16	Co@C	none	62	52 (40) <sup>c</sup>
17	Phen@C	none	8	4
18	Co@vul (Beller catalyst)	none	25	21
19	Stahl catalyst	none	18	15

[a] Reaction conditions: **1a** (0.50 mmol), cat. Co-Phen@C (6 mol%), *t*-BuOK (4 mol%) and *n*-decane (2 mL) heated at 150 °C for 36 h under argon atm. [b] Yields of **2a** and the conversion of **1a** are based on GC using *m*-xylene as an internal standard. [c] Yields in parentheses are based on isolated yields. [d] Reaction under homogeneous condition using *in-situ* generated Co-catalyst by reacting 1:1 mixture of Co-salt and 1,10-phenanthroline (Phen) followed by treatment with *t*-BuOK (4 mol%).

Table 2. Reusable cobalt-catalyzed direct quinoline synthesis via ADH: Scope of tetrahydroquinolines.<sup>[a]</sup>

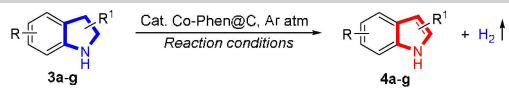
Entry	Substrate	Product	Conversion (%) <sup>[b]</sup>	Yield (%) <sup>[c]</sup>
1	<b>1a</b>	<b>2a</b>	100	93
2	<b>1b</b>	<b>2b</b>	99	94
3	<b>1c</b>	<b>2c</b>	95	91
4	<b>1d</b>	<b>2d</b>	100	97
5	<b>1e</b>	<b>2e</b>	96	92
6	<b>1f</b>	<b>2f</b>	100	98
7	<b>1g</b>	<b>2g</b>	85	78
8	<b>1h</b>	<b>2h</b>	100	95
9	<b>1i</b>	<b>2i</b>	100	80
10	<b>1j</b>	<b>2j</b>	58	54
11	<b>1k</b>	<b>2k</b>	64	57

[a] Reaction conditions: **1a–k** (0.50 mmol), cat. Co-Phen@C (6 mol%), *t*-BuOK (4 mol%), and *n*-decane (2 mL) heated at 150 °C (bath-temperature) for 36 h under open argon atm. [b] Based on GC. [c] Isolated yields.

with electron-rich, and electron-deficient substituents afforded the corresponding dehydrogenated products in good to excellent yields. Under standard reaction conditions, the unsubstituted THQ **1a** afforded the dehydrogenated product **2a** in 93% isolated yield (Table 1, entry 1) and THQs with electron-donating groups such as –Me, –OMe gave the desired products **2b–2e** in excellent yields of up to 97% (Table 2, entries 2–5). Notably, the substrate **1f** with a phenolic group (Ar-OH) underwent dehydrogenation smoothly and gave the expected product **2f** in 98% of isolated yield (Table 2, entry 6). Similarly, substrates such as 6-FTHQ, 6-BrTHQ, and 7-NO<sub>2</sub>THQ having electron-deficient groups were well tolerated and underwent ADH reaction to offer the corresponding N-heteroaromatics in excellent yields (up to 95%) with the liberation of H<sub>2</sub> gas (Table 1, entries 7–9). However, the 2-aryl substituted THQ derivatives **1j** and **1k** gave moderate yields under the optimized conditions (Table 1, entries 10–11). The low reactivity of **1j** and **1k** may be because products from these substrates can also C–H activate to give kappa2-phenylpyridine ligands that interfere with catalysis.

Next, the scope of the ADH strategy was successfully applied for the direct synthesis of indole derivatives (Table 3), a class of highly important pharmaceutically and biologically active motif. It was found that the electronic nature of the substrates had no significant effect on the ADH reaction under our cobalt catalyzed conditions. The unsubstituted indoline **3a**

**Table 3.** Reusable Cobalt catalyzed indole synthesis via ADH: Scope of indolines.<sup>[a]</sup>



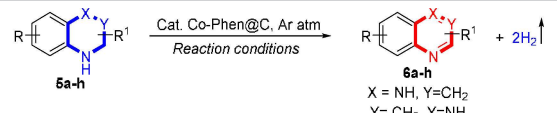
Entry	Substrate	Product	Conversion (%) <sup>b</sup>	Yield (%) <sup>c</sup>
1			100	98
2			94	90
3			97	93
4			97	92
5			93	88
6			100	96
7			100	98

[a] Reaction conditions: **3a–g** (0.50 mmol), cat. Co-Phen@C (6 mol%), *t*-BuOK (4 mol%), and *n*-decane (2 mL) heated at 150 °C (bath-temperature) for 36 h under open argon atm. [b] Based on GC. [c] Isolated yields.

and dihydroazaindole **3b** gave excellent yields of the corresponding dehydrogenated products **4a** and **4b** in 98% and 90%, respectively (Table 3 entries 1–2). The electron-rich indolines with –Me or –OMe groups gave the desired products **4c** in 93% and **4d** in 92% yields (Table 3 entries 3–4). The substrate **3e** with an electron-deficient ester group offered **4e** in 88% isolated yield (Table 3, entry 5). Notably, substrates with sensitive functional groups such as **3f** with an acid group and **3g** with bromo substituent underwent ADH reaction smoothly and yielded the expected products in excellent yields of up to 98% (Table 3, entries 6–7).

Inspired by the excellent results obtained for THQs and indolines, the present heterogeneous Co-catalyzed ADH protocol was applied for the synthesis of other N-heteroaromatics such as isoquinoline **6a**, anthracene **6b**, benzo[h]quinolone **6c** and indeed, good to excellent yields were obtained under the optimal conditions (Table 4 entries 1–3). Interestingly, the sterically hindered 2-phenyl-1,2,3,4-tetrahydroquinoxaline **5d** and 2-aryl substituted 1,2,3,4-tetrahydroquinazoline substrates also

**Table 4.** Reusable cobalt catalyzed ADH reaction: Scope of other N-heterocycles.<sup>[a]</sup>

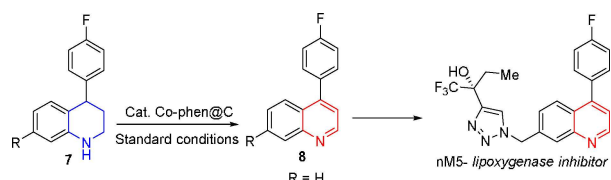


Entry	Substrate	Product	Conversion (%) <sup>b</sup>	Yield (%) <sup>c</sup>
1			97	93
2			93	89
3			78	74
4			100	96
5			99	96
6			95	91
7			100	94
8			100	93

[a] Reaction conditions: **5a–h** (0.50 mmol), cat. Co-Phen@C (6 mol%), *t*-BuOK (4 mol%), and *n*-decane (2 mL) heated at 150 °C (bath-temperature) for 36 h under open argon atm. [b] Based on GC. [c] Isolated yields.

underwent ADH reaction to offer the corresponding dehydrogenated products in excellent yields (products **6d** in 96%, **6e** in 96%, **6f** in 91% and **6g** in 94% yields). The substrate **5h** with a hexyl group at second position underwent catalytic dehydrogenation smoothly and gave the desired product **6h** in 93% yield.

Next, we have successfully applied our catalytic system for the preparation of drug intermediate. Thus, the pharmaceutically active intermediate **8** was prepared in good yield under our heterogeneous cobalt catalysed conditions (Scheme 2).



**Scheme 2.** Application in the synthesis of pharmaceutically active intermediate.

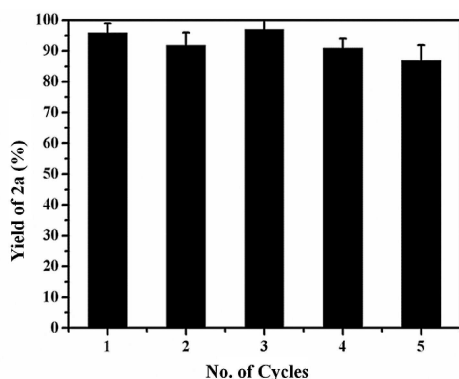
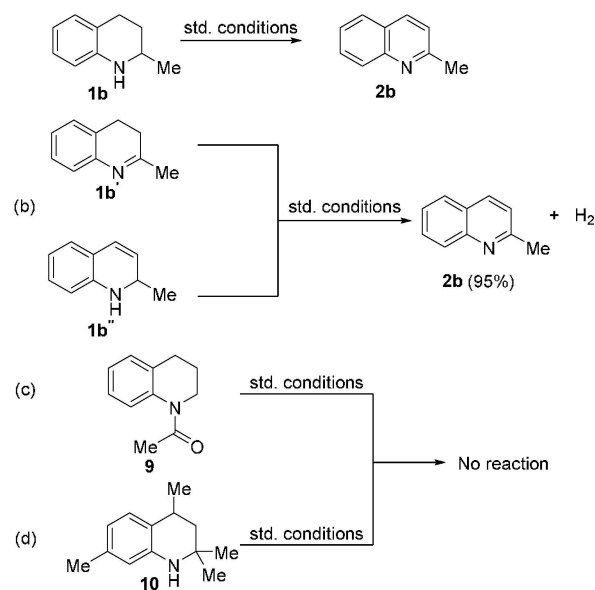


**Figure 6.** Reusability of the Co-Phen@C catalyst.

It is noteworthy that the present the Co-Phen@C catalyst was easily separated from the reaction medium and reused at least for five cycles without a considerable loss in its activity (Figure 6). This suggests that the catalyst is highly robust and does not undergo deactivation during catalysis. To confirm the heterogeneity of the catalyst, a hot filtration test was carried out. It was observed that after catalyst removal from the reaction mixture (48% yield of **2a**) there was no further increase in product yield. Notably, no product formation (trace) was observed under complete homogeneous reaction conditions (Table 1, entry 10). All these results clearly revealed that the present Co-catalysis truly is heterogeneous in nature.

To get insight into the mechanisms, several control experiments were carried out (Scheme 3). The presence of radical scavenger (butylated hydroxytoluene (BHT)) does not affect the reactivity of the catalyst, and the dehydrogenated product **2b** was isolated in 86% yield. This result ruled out a possibility of radical mechanism. In addition, when a partially dehydrogenated products **1b'** and **1b''** were subjected under standard

(a) Presence of radical scavenger

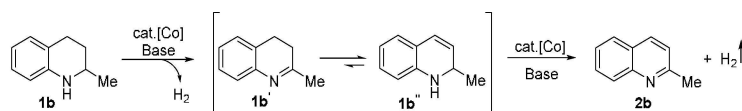


**Scheme 3.** Control experiments.

reaction conditions lead to **2b** in excellent yield (94% yield from **1b'** and 96% yield from **1b''**). This result indicates that the ADH reaction proceeds *via* the intermediate **1a'** which further undergoes isomerization reaction and lead to partially hydrogenated NH intermediate (**1b''**) and subsequent dehydrogenation leads to product **2b**. When *N*-protected substrate **9** and substrate **10** without an  $\alpha$ -H, were subjected to the present Co-catalysis, no dehydrogenated product was formed. These experiments suggest that a proton on N-atom and the  $\alpha$ -H of the C-2 position of the cyclic system are crucial for this reaction.

Based on the above results, we propose that the partially saturated N-heterocycles (**1**) bind to the cobalt surface through nitrogen center. This substrate binding has been accelerated by the base *t*-BuOK. Then, the surface-bound N-heterocycles undergo dehydrogenation reaction to give the intermediate (type **1b'**) with the liberation of one molecule of hydrogen. The intermediate **1b'** can undergo isomerization followed by subsequent dehydrogenation of another hydrogen molecule to give the complete dehydrogenated product **2b** (Scheme 4). The formation of H<sub>2</sub> gas was qualitatively observed in gas chromatography and also quantified.

In the context of 'hydrogen storage', the microscopic reversible hydrogenation reaction is also equally important. Despite significant progress in the development of catalytic reversible dehydrogenation/hydrogenation of N-heterocycles (e.g. quinolines) by molecularly defined homogeneous complexes, catalysts based on reusable non-noble metals is highly desired; however, rarely reported.<sup>[32]</sup> Very recently, research groups of Wang, and Li reported<sup>[32b]</sup> an ordered porous nitrogen-doped carbon matrix with atomically dispersed cobalt sites as an efficient catalyst for both dehydrogenation of N-heterocycles to release hydrogen and the reverse transfer hydrogenation of N-heterocycles to store hydrogen using formic acid



Scheme 4. Proposed catalytic pathway for the ADH of **1b**.

as a H<sub>2</sub> source (only one example). Inspired by our dehydrogenation results, we have investigated catalytic activity of nano cobalt-catalyst for hydrogenation of N-heteroarenes to the corresponding N-heterocycles using hydrogen as a reductant.

We further explored hydrogenation of quinoline derivatives to the corresponding tetrahydroquinoline derivatives. Thus, hydrogenation of quinolines (**2**) under hydrogen pressure selectively led to quinolines in excellent yields simply by using the same nano cobalt-catalyst (Table 5). The catalyst was reused and had shown excellent activity even after 4<sup>th</sup> cycle. Inspired by the excellent results obtained for hydrogenation of THQs, the present heterogeneous Co-catalyst was successfully applied for the hydrogenation of other N-heteroaromatics such as indoline, isoquinoline, quinazoline, quinoxaline, and anthracene derivatives and indeed, good to excellent yields of the hydrogenated products were obtained under the optimal conditions.

To investigate the active phase of the present heterogeneous cobalt-catalyst, we have carried out the reaction with the individual phases (Table S2 in Supporting Information). From the experimental results, it is clear that none of the individual phase of cobalt is active for the reactivity. The specific structure of Co-Phen@C catalyst is responsible for such kind of catalysis. The above morphology is very much similar to the cobalt

catalyst reported by Beller and co-workers wherein core is made up of metallic cobalt while the shell is made up of cobalt oxide (as cobalt present in shell got oxidized to form cobalt oxide).<sup>[12a]</sup> It is important to note that the availability of different active sites with different nature in close proximity helps to carry out such complex heterogeneous catalytic reactions. Thus, we believe that all elementary reactions like, hydrogen adsorption, hydrogen dissociation, N-heterocycle adsorption, subsequent reaction, desorption of products, should occur in tandem for such complex reactions.<sup>[33]</sup> Thus, mixed interphase in Co-Phen@C catalyst helps in the present catalysis.

## Conclusions

In summary, we have developed highly efficient, robust and reusable cobalt-based nanocatalyst for reversible dehydrogenation and hydrogenation of N-heterocycles. Both the acceptorless dehydrogenation and the hydrogenation processes catalyzed by a single reusable cobalt-catalyst, and operates under mild, benign conditions. The present nano-catalyst performs excellently with several recycling test. The synthetic utility of the present nanocobalt catalyzed ADH reaction is demonstrated explicitly to the pharmaceutically relevant molecule.

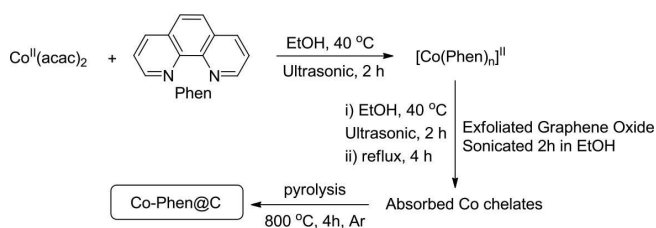
## Experimental Section

### Synthesis of Co-Phen@C

In a 100 mL beaker Co(II)acetylacetonate precursor (0.5 mmol) and 1,10-phenanthroline ligand (0.5 mmol) were dissolved in 30 mL of ethanol and sonicated for 2 h to form Co-phenanthroline complex. In another 250 mL beaker 560 mg of EGO support was taken in 70 mL of ethanol and sonicated for 2 h. The above obtained EGO suspension and Co-phenanthroline complex solution were mixed together in 250 mL beaker and further sonicated for 2 h. The suspension was refluxed at 85 °C for 4 h and after cooling down to room temperature ethanol was evaporated in vacuum. The solid sample obtained was dried at 80 °C for 14 h. Then, it was ground to a fine powder followed by calcination at 800 °C under a stream of argon with the flow rate of 30 mL/min and the heating rate: 25 °C/min for about 4 h to obtain a catalyst Co-Phen@C (Scheme 5). For the synthesis of other conventional based supports (SiO<sub>2</sub>, TiO<sub>2</sub>, Al<sub>2</sub>O<sub>3</sub>) synthesis of Co-Phen@SiO<sub>2</sub>, Co-Phen@TiO<sub>2</sub> and Co-Phen@Al<sub>2</sub>O<sub>3</sub> catalysts were done using 560 mg of the respective support. Other steps in the synthesis were identical as per explained in the synthesis of Co-Phen@C.

Table 5. Cobalt catalyzed hydrogenation of quinolines using H <sub>2</sub> . <sup>[a]</sup>	
Scope of Quinolines:	
	98%
	88%
	95% (89%) <sup>b</sup>
	80%
	89%
	92%
Scope of other N-Heterocycles:	
	77%
	96%
	71%
	89%
	93%

[a] Reaction conditions: Quinolines (0.3 mmol), cat. Co-Phen@C (50 mg), 500 psi H<sub>2</sub>, and toluene (2 mL) heated at 120 °C (bath-temperature) for 72 h under open argon atm and the yields are isolated yields. [b] After 4<sup>th</sup> cycle.



Scheme 5. Synthesis procedure of Co-Phen@C catalyst.

### Catalyst Characterization

**PXRD:** Powder XRD samples were analyzed on an Xpert Pro model PAN analytical diffractometer from Philips PAN analytical X'PRET PRO instruments operated at a voltage of 40 kV and a current of 30 mA with Cu K $\alpha$  radiation ( $\lambda = 1.5406 \text{ \AA}$ ). The samples were scanned in a  $2\theta$  range from  $10^\circ$  to  $80^\circ$  with a scan rate of  $0.39^\circ$  per minute.

**TEM:** Samples dissolved in ethanol was drop cast onto separate 200 mesh carbon coated copper grids and studied using a transmission electron microscope (TEM, FEI model TECNAI G2 F20) operating at an accelerating voltage of 200 kV.

**Electron Dispersive X-ray Analysis:** Energy dispersive X-ray analysis (EDX) measurements on the cobalt supported graphene sample of the active catalyst was performed using transmission electron microscope (TEM, FEI model TECNAI G2 F20) operating at an accelerating voltage of 200 kV.

**ICP analysis:** Inductively coupled plasma atomic emission spectroscopy (ICP-AES) were acquired for the elemental analysis of absolute cobalt content within the sample. Analysis performed by SPECTRO analytical instruments GmbH, model ARCOS simultaneous ICP spectrometer, Germany.

**Raman analysis:** LabRam spectrometer (HJY, France) was used for Raman analysis with a laser wavelength of 632 nm.

**X-ray Photoelectron spectroscopy:** XPS surface investigation has been performed on the PHI 5000 VersaProbe II XPS system (Physical Electronics) with a monochromatic Al-K $\alpha$  source (15 kV, 50 W) and photon energy of 1486.7 eV. Dual beam charge compensation was used for all measurements. All the spectra were measured in the vacuum of  $1.3 \times 10^{-7}$  Pa and at the room temperature of  $21^\circ\text{C}$ . The analyzed area on each sample was a spot of  $200 \mu\text{m}$  in diameter. The spectra were evaluated with the MultiPak (Ulvac - PHI, Inc.) software. All binding energy (BE) values were referenced to the carbon peak C 1s at 284.80 eV.

### TEM, HRTEM-Elemental Mapping

Microscopic TEM images were obtained by HRTEM TITAN 60-300 with X-FEG type emission gun, operating at 80 kV. This microscope is equipped with Cs image corrector and a STEM high-angle annular dark-field detector (HAADF). The point resolution is 0.06 nm in TEM mode. The elemental mappings were obtained by STEM-energy dispersive X-ray spectroscopy (EDS) with acquisition time 20 min. For HRTEM analysis, the powder samples were dispersed in ethanol and ultrasonicated for 5 min. One drop of this solution was placed on a copper grid with holey carbon film.

**GC Analysis:** The conversion and selectivity of the reactions were analyzed by GC employing chromatograph Agilent 6820 (Agilent, United States), equipped with flame ionization detector (FID) and chromatographic column DB5 ( $30 \times 0.250 \times 0.25$ ). The following

experimental parameters were applied: initial temperature of  $100^\circ\text{C}$ , increased to  $250^\circ\text{C}$  with a rate of  $10^\circ\text{C}/\text{min}$ .

### General Procedure for the Acceptorless Dehydrogenation of N-Heterocycles

To an oven dried Schlenk tube (25 mL), Co-Phen@C (28 mg, 6 mol%), *t*-BuOK (4 mol%), N-heterocycles (0.5 mmol), *n*-decane (2 mL) were added under argon atmosphere. The solution was refluxed at  $150^\circ\text{C}$  with stirring under open argon flow for 36 h. After cooling down the reaction mixture to room temperature the catalyst was separated from the reaction mixture by centrifugation and the reaction mixture was analyzed by GC and GC-MS. The supernatant was transferred into another flask, and the catalyst was washed with EtOAc ( $2 \times 4$  mL) and the washings were collected. The solvent was evaporated from the reaction mixture, and the crude product was subjected to silica gel column chromatography using EtOAc : petroleum ether to afford the desired product.

### General Procedure for the Hydrogenation of N-Heteroarenes

In a reaction vial (5 mL), N-heteroarenes (0.3 mmol) with Co-Phen@C (50 mg) were mixture in 2 mL of toluene. The closed reaction vials were placed into a 300 mL autoclave via a prepared metal plate. The autoclave was flushed with hydrogen gas twice and pressurized with hydrogen. Then, the autoclave was placed into an aluminum block at  $120^\circ\text{C}$  for 60 h. After the reaction was complete, the autoclave was cooled to room temperature and the hydrogen was released. The crude reaction mixture was purified by column chromatography on silica to afford corresponding hydrogenated products.

### Supporting Information

The Supporting Information includes XPS of C1s spectra, Raman spectra, SAED patterns, and EDX analysis of Co-Phen@C catalyst, experimental and spectroscopic data, mechanistic studies, and copies of  $^1\text{H}$ , and  $^{13}\text{C}$  NMR spectra (PDF).

### Author Contributions

The manuscript was written through contributions of all authors. All authors have given approval to the final version of the manuscript.

### Acknowledgements

This research work was supported by IISER-Tirupati and SERB, India (Grant No: CRG/2018/002480/OC). Authors thank CSIR-NCL for providing experimental and infrastructure facilities. MS thanks to the UGC, India for fellowship. EB thanks Manoj B. Gawande (Palacký University, Czech Republic) for XPS analysis.

### Conflict of Interest

The authors declare no conflict of interest.

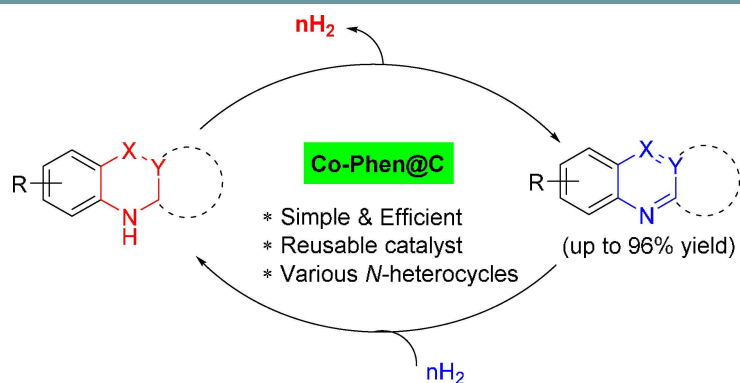


**Keywords:** Cobalt catalyst · N-heterocycles · Acceptorless dehydrogenation · Hydrogenation · Heterogeneous catalysis

- [1] a) S. Süzen, *Bioactive Heterocycles V*, Springer **2007**, 145. b) E. Vitaku, D. T. Smith, J. T. J. Njardarson, *Med. Chem.* **2014**, *57*, 10257.
- [2] a) P. Jessop, *Nat. Chem.* **2009**, *1*, 350; b) R. H. Crabtree, *Energy Environ. Sci.* **2008**, *1*, 134; c) E. Clot, O. Eisenstein, R. H. Crabtree, *Chem. Commun.* **2007**, 2231; d) P. Hu, E. Fogler, Y. Diskin-Posner, M. A. Iron, D. A. Milstein, *Nat. Commun.* **2015**, *6*, 6859.
- [3] G. E. Dobreiner, R. H. Crabtree, *Chem. Rev.* **2010**, *110*, 681.
- [4] a) P. P. Fu, R. G. Harvey, *Chem. Rev.* **1978**, *78*, 317. b) D. R. Buckle, John Wiley & Sons, Inc.: New York, **2010**.
- [5] G. W. Gribble, T. L. Gilchrist, *Prog. Heterocycl. Chem.*, ed. Pergamon, Oxford, **2005**, *15*, 167.
- [6] D. R. Buckle, John Wiley & Sons, Inc.: New York, **2010**.
- [7] L. Jr Que, W. B. Tolman, *Nature* **2008**, *455*, 333.
- [8] H. Yuan, W.-J. Yoo, H. Miyamura, S. Kobayashi, *J. Am. Chem. Soc.* **2012**, *134*, 13970.
- [9] K. Yamaguchi, N. Mizuno, *Angew. Chem. Int. Ed.* **2003**, *42*, 1480.
- [10] D. Ge, L. Hu, J. Wang, X. Li, F. Qi, J. Lu, X. Cao, H. Gu, *ChemCatChem* **2013**, *5*, 2183.
- [11] S. Furukawa, A. Suga, T. Komatsu, *Chem. Commun.* **2014**, *50*, 3277.
- [12] a) X. Cui, Y. Li, S. Bachmann, M. Scalone, A.-E. Surkus, K. Junge, C. Topf, M. Beller, *J. Am. Chem. Soc.* **2015**, *137*, 10652; b) A. V. Iosub, S. S. Stahl, *Org. Lett.* **2015**, *17*, 4404; c) S. Biswas, B. Dutta, K. Mullick, C.-H. Kuo, A. S. Poyraz, S. L. Suib, *ACS Catal.* **2015**, *5*, 4394.
- [13] W. Yao, Y. Zhang, X. Jia, Z. Huang, *Angew. Chem. Int. Ed.* **2014**, *53*, 1390.
- [14] Recent representative reviews on acceptorless dehydrogenation reactions: a) N. Gorgas, K. Kirchner, *Acc. Chem. Res.* **2018**, *51*, 1558; b) K. Sordakis, C. Tang, L. K. Vogt, H. Junge, P. J. Dyson, M. Beller, G. Laurenczy, *Chem. Rev.* **2018**, *118*, 372; c) G. A. Filonenko, R. V. Putten, E. J. M. Hensen, E. A. Pidko, *Chem. Soc. Rev.* **2018**, *47*, 1459. d) R. H. Crabtree, *Chem. Rev.* **2017**, *117*, 9228; e) E. Balaraman, A. Nandakumar, G. Jaiswal, M. K. Sahoo, *Catal. Sci. Technol.* **2017**, *7*, 3177; f) A. Kumar, T. M. Bhatti, A. S. Goldman, *Chem. Rev.* **2017**, *117*, 12357; g) V. S. Thoi, Y. Sun, R. J. Long, C. J. Chang, *Chem. Soc. Rev.* **2013**, *42*, 2388; h) C. Gunanathan, D. Milstein, *Science* **2013**, *341*, 1229712; i) J. Choi, A. H. R. MacArthur, M. Brookhart, A. S. Goldman, *Chem. Rev.* **2011**, *111*, 1761.
- [15] a) R. H. Crabtree, *Energy Environ. Sci.* **2008**, *1*, 134; b) L. Schlappbach, A. Züttel, *Nature* **2001**, *414*, 353.
- [16] a) E. Clot, O. Eisenstein, R. H. Crabtree, *Chem. Commun.* **2007**, *22*, 2231; b) A. Moores, M. Poyatos, Y. Luo, R. H. Crabtree, *New J. Chem.* **2006**, *30*, 1675; c) Y. Cui, S. Kwok, A. Buchholtz, B. Davis, R. A. Whitney, P. G. Jessop, *New J. Chem.* **2008**, *32*, 1027.
- [17] a) M. Amende, C. Gleichweit, K. Werner, S. Schernich, W. Zhao, M. P. A. Lorenz, O. Höfert, C. Papp, M. Koch, P. Wasserscheid, M. Laurin, H.-P. Steinrück, J. Libuda, *ACS Catal.* **2014**, *4*, 657; b) D. Forberg, T. Schwob, M. Zaheer, M. Friedrich, N. Miyajima, R. Kempe, *Nat. Commun.* **2016**, *7*, 13201–13206; c) S. Kato, Y. Saga, M. Kojima, H. Fuse, S. Matsunaga, A. Fukatsu, M. Kondo, S. Masaoka, M. Kanai, *J. Am. Chem. Soc.* **2017**, *139*, 2204; d) M. Zheng, J. Shi, T. Yuan, X. Wang, *Angew. Chem. Int. Ed.* **2018**, *57*, 5487.
- [18] a) K. H. He, F. Tan, C. Z. Zhou, G. J. Zhou, X. L. Yang, Y. Li, *Angew. Chem. Int. Ed.* **2017**, *129*, 3080; b) M. G. Manas, L. S. Sharninghausen, E. Lin, R. H. Crabtree, *J. Organomet. Chem.* **2015**, *792*, 184; c) D. Talwar, A. Gonzalez-de-Castro, H. Y. Li, J. Xiao, *Angew. Chem. Int. Ed.* **2015**, *54*, 5223; d) M. Kojima, M. Kanai, *Angew. Chem. Int. Ed.* **2016**, *55*, 12224; e) H. Li, J. Jiang, G. Lu, F. Huang, Z. X. Wang, *Organometallics* **2011**, *30*, 3131.
- [19] a) R. Yamaguchi, C. Ikeda, Y. Takahashi, K.-i. Fujita, *J. Am. Chem. Soc.* **2009**, *131*, 8410; b) J. Wu, D. Talwar, S. Johnston, M. Yan, J. Xiao, *Angew. Chem. Int. Ed.* **2013**, *52*, 6983; c) K. i. Fujita, Y. Tanaka, M. Kobayashi, R. Yamaguchi, *J. Am. Chem. Soc.* **2014**, *136*, 4829; d) S. Chakraborty, W. W. Brennessel, W. D. Jones, *J. Am. Chem. Soc.* **2014**, *136*, 8564; e) R. Xu, S. Chakraborty, H. Yuan, W. D. Jones, *ACS Catal.* **2015**, *5*, 6350; f) M. Kojima, M. Kanai, *Angew. Chem.* **2016**, *128*, 12412; g) K. H. He, F. F. Tan, C. Z. Zhou, G. J. Zhou, X. L. Yang, Y. Li, *Angew. Chem. Int. Ed.* **2017**, *56*, 3080.
- [20] a) H. Yuan, W. J. Yoo, H. Miyamura, S. Kobayashi, *J. Am. Chem. Soc.* **2012**, *134*, 13970; b) K. Yamaguchi, N. Mizuno, *Angew. Chem. Int. Ed.* **2003**, *42*, 1480; c) F. Li, J. Chen, Q. Zhang, Y. Wang, *Green Chem.* **2008**, *10*, 553; d) M. H. So, Y. Liu, C. M. Ho, C. M. Che, *Chem. Asian J.* **2009**, *4*, 1551; e) H. Choi, M. P. Doyle, *Chem. Commun.* **2007**, *7*, 745; f) D. V. Jawale, E. Gravel, N. Shah, V. Dauvois, H. Li, I. N. N. Namboothiri, E. Doris, *Chem. Eur. J.* **2015**, *21*, 7039; g) K. Yamaguchi, N. Mizuno, *Chem. Eur. J.* **2003**, *9*, 4353.
- [21] a) G. Jaiswal, V. G. Landge, D. Jagadeesan, E. Balaraman, *Nat. Commun.* **2017**, *8*, 2147; b) G. Jaiswal, V. G. Landge, D. Jagadeesan, E. Balaraman, *Green Chem.* **2016**, *18*, 3232.
- [22] a) H. Fei, J. Dong, M. J. Arellano-Jiménez, G. Ye, N. Dong Kim, E. L. G. Samuel, Z. Peng, Z. Zhu, F. Qin, J. Bao, M. J. Yacaman, P. M. Ajayan, D. Chen, J. M. Tour, *Nat. Commun.* **2015**, *6*, 8668; b) A. V. Iosub, S. S. Stahl, *Org. Lett.* **2015**, *17*, 4404.
- [23] D. Formenti, F. Ferretti, C. Topf, A.-E. Surkus, M.-M. Pohl, J. Radnik, M. Schneider, K. Junge, M. Beller, F. Ragaini, *J. Catal.* **2017**, *351*, 79.
- [24] Á. Vivancos, M. Beller, M. Albrecht, *ACS Catal.* **2017**, *8*, 17.
- [25] a) C. Deraedt, R. Ye, W. T. Ralston, F. D. Toste, G. A. Somorjai, *J. Am. Chem. Soc.* **2017**, *139*, 18084; b) J.-W. Zhang, D.-d. Li, G.-p. Lu, T. Deng, C. Cai, *ChemCatChem* **2018**, *10*, 4966.
- [26] a) D. Yuan, T. G. Martha, Z. Chi, Chi, L. Jian, *Nanotechnology* **2017**, *28*, 505602; b) J. Lu, L. Yang, B. Xu, Q. Wu, D. Zhang, S. Yuan, Y. Zhai, X. Wang, Wang, Y. Fan, Z. Hu, *ACS Catal.* **2014**, *4*, 613.
- [27] C. D. Wager, M. W. Riggs, L. E. Davis, J. F. Moulder, G. E. Mullenberg, *Handbook of X-Ray Photoelectron Spectroscopy* (Perkin-Elmer, Eden Prairie, MN, **1979**).
- [28] S. A. Needham, G. X. Wang, K. Konstantinov, Y. Tournayre, Z. Lao, H. K. Liu, *Electrochem. Solid-State Lett.* **2006**, *9*, A315.
- [29] a) R. V. Jagadeesh, H. Junge, M.-M. Pohl, Jr. Radnik, A. Brückner, M. Beller, *J. Am. Chem. Soc.* **2013**, *135*, 10776; b) E. S. Andreiadis, P.-A. Jacques, P. D. Tran, A. Leyris, M. Chavarot-Kerlidou, B. Jousseme, M. Matheron, J. Păcaut, S. Palacin, M. Fontecave, V. Artero, *Nat. Chem.* **2013**, *5*, 48; c) K. P. Reddy, R. Jain, M. K. Ghosalya, C. S. Gopinath, *J. Phys. Chem. C* **2017**, *121*, 21472.
- [30] a) J. R. Pels, F. Kapteijn, J. A. Moulijn, Q. Zhu, K. M. Thomas, *Carbon* **1995**, *33*, 1641; b) S. Stankovich, D. A. Dikin, R. D. Piner, K. A. Kohlhaas, A. Kleinhammes, Y. Jia, Y. Wu, S. T. Nguyen, R. S. Ruoff, *Carbon* **2007**, *45*, 1558.
- [31] a) A. Ganguly, S. Sharma, P. Papakonstantinou, J. Hamilton, *J. Phys. Chem. C* **2011**, *115*, 17009; b) D. Yang, A. Velamakanni, G. Bozoklu, S. Park, M. Stoller, R. D. Piner, S. Stankovich, I. Jung, D. A. Field, C. A. Ventrice, R. S. Ruoff, *Carbon* **2009**, *47*, 145.
- [32] a) K. Kaneda, Y. Mikami, T. Mitsudome, T. Mizugaki, K. Jitsukawa, *Heterocycles* **2010**, *82*, 1371; b) Y. Han, Z. Wang, R. Xu, W. Zhang, W. Chen, L. Zheng, J. Zhang, J. Luo, K. Wu, Y. Zhu, C. Chen, Q. Peng, Q. Liu, P. Hu, D. Wang, Y. Li, *Angew. Chem. Int. Ed.* **2018**, *57*, 11262.
- [33] a) R. Jain, C. S. Gopinath, *ACS Appl. Mater. Interfaces* **2018**, *10*, 41268; b) T. Mathew, K. Sivarajani, E. S. Gnanakumar, Y. Yamada, T. Kobayashi, C. S. Gopinath, *J. Mater. Chem.* **2012**, *22*, 13484; c) T. Mathew, N. R. Shiju, K. Sreekumar, B. S. Rao, C. S. Gopinath, *J. Catal.* **2002**, *210*, 405.

Manuscript received: February 28, 2019  
Revised manuscript received: April 6, 2019  
Version of record online: ■■■, ■■■■

## FULL PAPERS



G. Jaiswal, M. Subaramanian, M. K. Sahoo, Prof. E. Balaraman\*

1 – 10

**A Reusable Cobalt Catalyst for Reversible Acceptorless Dehydrogenation and Hydrogenation of N-Heterocycles**



**Simple, efficient and mild:** An efficient reusable cobalt-based heterogeneous catalyst for reversible dehydrogenation and hydrogenation of N-

heterocycles is reported. Both processes are catalyzed by a single reusable cobalt-catalyst that operates under mild and benign conditions.